Available online at www.sciencedirect.com
SCIENCE DIRECT
Trans. Nonferrous Met. Soc. China 16(2006) 414−420
Transactions of Nonferrous Metals Society of China
www.csu.edu.cn/ysxb/

Zincate mechanism on cast Al-Si alloy in non-cyanide multi-metal zincate solutions

HUANG Xiao-mei(黄晓梅), LI Ning(李 宁), LI De-yu(黎德育), JIANG Li-min(蒋丽敏)

Department of Applied Chemistry, Harbin Institute of Technology, Harbin 150001, China

Received 19 August 2005; accepted 18 November 2005

Abstract: Arrhenius formula was applied to calculate the apparent activation energy of zincate reaction. The standard electrode potential of all the metal coordinating ions and the order of galvanic couple of different metals in zincate solution were also calculated. Electrochemical behavior of zincate process was studied by Tafel polarization curves, *E*—*t* curves, and electrochemical impedance spectroscopy(EIS). The results show that the apparent activation energy of zincate reaction in non-cyanide multi-metal zincate solution is smaller than that in simple zincate solution, and precipitation sequence of all the metals in zincate solution is Cu, Ni, Fe and Zn. Relationship between the potential at 30 s before zincate and coverage was attained according to the change of potential of zincate. EIS shows that inductive reactance is produced during zincate.

Key words: cast Al-Si alloy; non-cyanide multi-metal zincate; zincate solution; zincate mechanism; apparent activation energy

1 Introduction

Si is an important element in Al-Si alloys, the content of which greatly affects the physical, mechanical and chemical properties of Al-Si alloys[1−3]. Due to special structure and cast techniques[4, 5], pre-treatment of cast Al-Si alloys before coating is difficult[6−8], and zincate is mainly applied at home and abroad at present[9-11]. LASHMORE[12] stated that zincate technique almost covered the whole market. STOYANOVA and STOYCHEV[13] researched zincate process on Al in alkaline media, and zincate mechanism was put forward by studying the kinetics of electrode reaction. PARAMASIVAM et al[15] and TANG et al[16] also studied the zincate mechanism successively, however, zincate mechanism on cast Al-Si alloys in non-cyanide multi-metal zincate solution was still not reported. Kinetics, thermodynamics and electrochemistry of zincate process in non-cyanide multi-metal zincate solution were systematically studied in this paper, and its zincate mechanism was also discussed.

2 Experimental

The A356 Al-Si alloy contained 7.5% Si, 0.3% Mg, 0.2% Cu, 0.2% Fe, 0.2% Ti, 0.1% Mn and 0.05% Ni(mass fraction). The main components of the non-cyanide multi-metal zincate solution were 110 g/L of NaOH, 18 g/L of Ni^{2+}, Cu^{2+}, Fe^{2+} and Zn^{2+}, 90 g/L of composite complexing agents, 4-6 g/L of additives. The zincate process was the same as elsewhere[17, 18].

Electrochemical tests of zincate process were carried out on CHI 660 Electrochemical Station, with Hg-HgO electrode(NaOH 2 mol/L) as reference electrode, and Pt electrode as counter electrode.

3 Results and discussion

3.1 Kinetics of zincate process

1) Calculation of zincate velocity

Zero-gravity was applied to measure the mass of zincate film, which operated as the difference of the mass of Al-Si alloy test piece after and before zincate process, ignoring the minute dissolved part of the base. The dissolved part could not be calculated accurately right now, which was substituted by the mass loss in NaOH solution with the same concentration of zincate solution. Mass variation curves during zincate process are shown in Fig.1.

It shows that mass increment of the test piece reaches its maximum at 30 s, and then a mass loss is detected. Zincate rate curves made from Fig.1 are shown

Corresponding author: HUANG Xiao-mei; Tel: +86-451-86413721; E-mail: huangxm@hit.edu.cn

in Fig.2, the macroscopic rate and corrosion rate of Al decrease with the increase of zincate time. From the beginning to 30 s, macroscopic rate and corrosion rate of Al decrease sharply, while after 30 s, they decrease gently, which may be due to the coverage of zinc layer on Al-Si alloy surface, thus the area for replacement reaction of Al and Zn is reduced. The growth rate of zinc reaches its maximum at 10 s, and decreases with the increase of zincate time. Macroscopic rate and deposit rate of Zn in simple zincate solution are larger than that in non-cyanide multi-metal zincate solution, indicating that the existence of multi-metal is beneficial for reducing the deposit rate of zinc, and attaining fine and even zinc crystals.

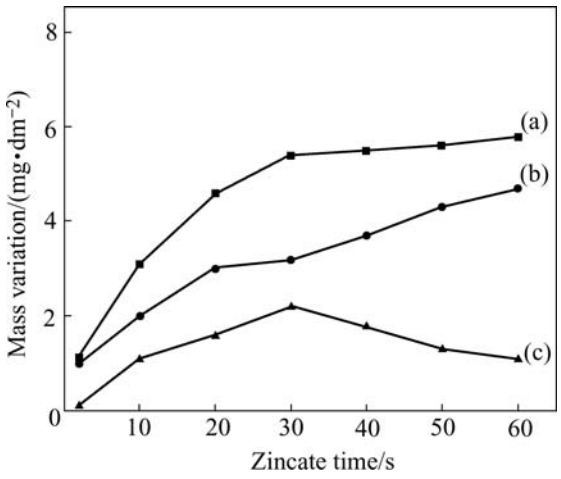

Fig.1 Mass variation curves during zincate process: (a) Mass variation curve of zincation layer; (b) Mass loss curve of substrate corrosion; (c) Measured mass of tested sample

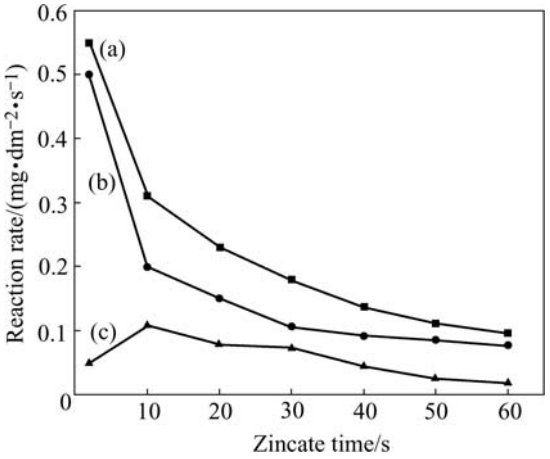

Fig.2 Zincate rate curves: (a) Macroscopic rate; (b) Corrosion rate of aluminum; (c) Growth rate of zinc deposition

2) Calculation of apparent activation energy E_a in zincate process

Assuming that the apparent activation energy E_a in zincate process is independent of the temperature, from the following Arrhenius formula:

$$\frac{\mathrm{d}\ln k}{\mathrm{d}T}=\frac{-E_a}{RT^2} \tag{1}$$

One can obtain

$$\ln k=-\frac{E_a}{RT}+B \tag{2}$$

Thus a straight line can be drawn between ln$k$ and $-1/T$. The apparent activation energy E_a can be calculated from the slope of the line. Zincate rate, k in this study is the mass of zinc layer per unit area and time. Relationship between the rate constant (ln$k$) of zincate and temperature is shown in Fig.3.

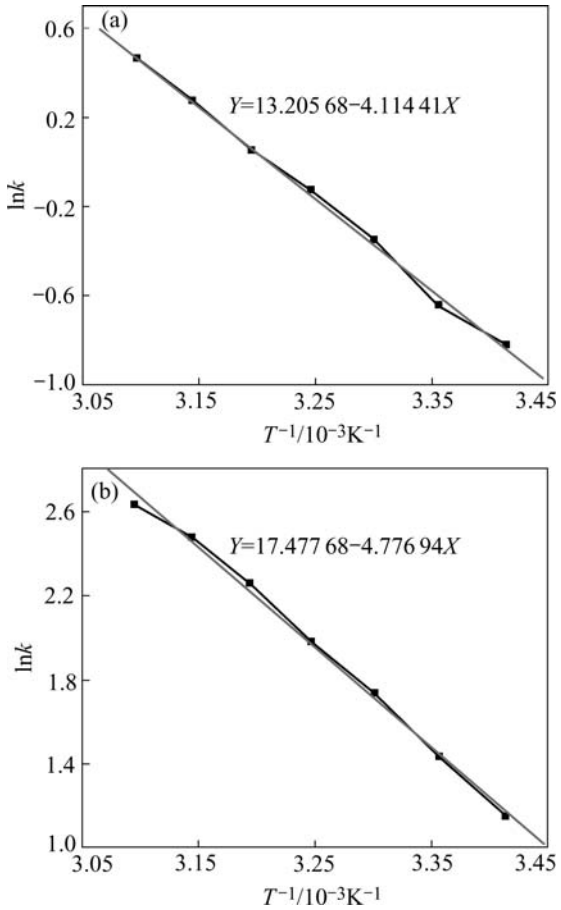

Fig.3 Relationship between zincate rate and temperature: (a) In multi-metal zincate solution; (b) In simple zincate solution

From linear fitting, the apparent activation energy E_a of zincate process in non-cyanide multi-metal zincate solution is 34.207 kJ/mol, while that in simple zincate solution is 39.716 kJ/mol, indicating that the existence of Cu, Fe, Ni ions and complexing agents in zincate solution makes zincate reaction easier.

3.2 Thermodynamics in zincate process

1) Standard electrode potential of metal ions in zincate solution and electromotive force of replacement

reaction

Ignoring the liberation of hydrogen, cathodic reaction in zincate process is the deposit of metal ions by obtaining electrons:

$$[ML_x]^n \rightarrow M^{2+} + xL^{(n-2)/2} \quad (3)$$

$$M^{2+} + 2e \rightarrow M \quad (4)$$

In formula (3), L represents the ligand, $[ML_x]^n$ is the complexing ions, x is the coordination number and n is the charge number of the complexing ions.

Stable complexing ions are formed from metal ions and complexing agents in strong alkaline solutions, thus electrode potential of the metals is different from that under standard conditions. Assume that zinc complexes with NaOH, Fe with seignette salt, Ni and Cu with sodium citrate.

Firstly, oxide film on the surface of Al-Si alloy was dissolved in strong alkaline zincate solution:

$$Al_2O_3 + 2NaOH = 2NaAlO_2 + H_2O \quad (5)$$

Then electrochemical reaction took place on the bare surface of Al-Si alloy:

$$2Al + 3[Zn(OH)_4]^{2-} \rightarrow 2AlO_2^- + 3Zn + 4H_2O + 4OH^- \quad (6)$$

$$E^0_{[Zn(OH)_4]^{2-}} = E^0_{Zn} - \frac{RT}{nF}\lg K =$$
$$-0.763 - 0.0295 \times 17.66 = 1.284\ V \quad (7)$$

where E^0_{Zn} is the standard reduction potential of Zn^{2+}, R is the gas constant, F is the Faraday constant and n is the electron transfer number in the reaction. The electromotive force of the zincate reaction in zincate solution containing complexing agents can be described as

$$\varepsilon^0 = E^0_{Cathodic} - E^0_{Anodic} = E^0_{[Zn(OH)_4]^{2-}} - E^0_{Al} =$$
$$-1.284 - (-2.3) = 1.016 \quad (8)$$

If $\varepsilon^0 > 0.3$V, formula (6) can take place spontaneously, Al on the surface of Al-Si alloy being replaced by Zn and a Zn layer formed. For multi-metal zincate solution, Fe, Ni and Cu can be deposited on the surface of Al-Si alloy together with Zn.

Standard electrode potential of complex ions and electromotive force in multi-metal zincate solution during replacement reaction are listed in Table 1.

In Table 1, E_s is the standard electrode potential, and E_c is the electrode potential of complex ions. Electromotive force reflects the impetus of the replacement reaction. The order of E_c is $E_c(Cu^{2+}) > E_c(Ni^{2+}) > E_c(Fe^{2+}) > E_c(Zn^{2+}) > 0.3$V, indicating that replacement reaction of Zn, Ni, Fe and Cu is possible. $E_c(Zn^{2+})$ is about 1 V, however, $E_c(Cu^{2+}) > E_c(Ni^{2+}) > E_c(Fe^{2+}) > 1.6$V, which means that replacement reaction in multi-metal zincate solution begins with Cu^{2+}, Ni^{2+}, Fe^{2+}, and then Zn^{2+} will be replaced.

Table 1 Standard electrode potential of complex ions and electromotive force in multi-metal zincate solution during replacement reaction

Metal ions	Complexing agents	lg$K$	E_s/V	E_c/V	ε^0/V
Zn^{2+}	NaOH	17.66	-0.76	-1.284	1.016
Fe^{2+}	Seignette salt	7.49	-0.44	-0.661	1.639
Ni^{2+}	Sodium citrate	6.90	-0.25	-0.454	1.846
Cu^{2+}	Sodium citrate	14.2	0.34	-0.079	2.221

2) Galvanic couple order of Al-Si alloy, Zn, Fe, Ni and Cu in muti-metal zincate solution

Tafel polarization curves of Al-Si alloy, Zn, Fe, Ni and Cu in alkaline multi-metal zincate solution are shown in Fig.4. The self-corrosion potential is taken as stable potential and then galvanic couple order is attained, shown in Table 2.

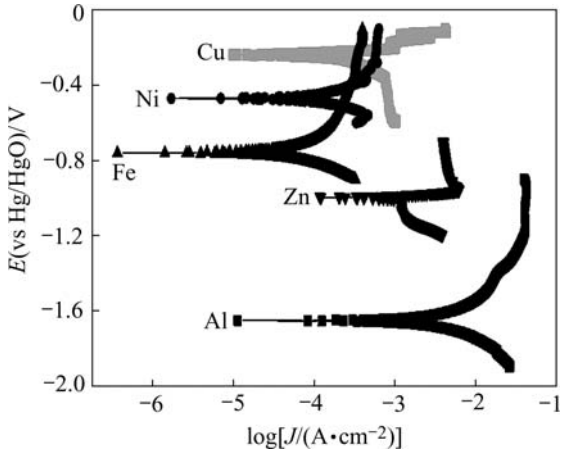

Fig.4 Tafel polarization curves of different metals in zincate solution

Table 2 Order of galvanic couple of different metals in zincate solution

Electrode	E_{corr}(vs Hg/HgO)/V
Cu	-0.238
Ni	-0.470
Fe	-0.760
Zn	-0.996
Al-Si alloy	-1.652

Galvanic couple order in zincate solution is Cu＞Ni＞Fe＞Zn, in consistent with theoretical values, thus the deposit order of the metals is Cu, Ni, Fe and then Zn. Film dissolution took place in the late period of zincate process, the potential being close to that of Zn, and Cu, Ni and Fe would not be dissolved due to their high potential. EDS and EPMA analyses of the components of zinc layer show higher content of Fe than Ni, which is similar to ‘abnormal co-deposition’ in electroplating and the deposit of Fe restrains the deposit of nickel.

3.3 Electrochemical study of zincate process

1) Tafel polarization curves of zinc layers in 3.5% NaCl solution

Tafel polarization curves of zinc layers on Al-Si alloy attained from non-cyanide multi-metal zincate solution were tested in 3.5% NaCl solution, as shown in Fig.5, and the fitting results are listed in Table 3.

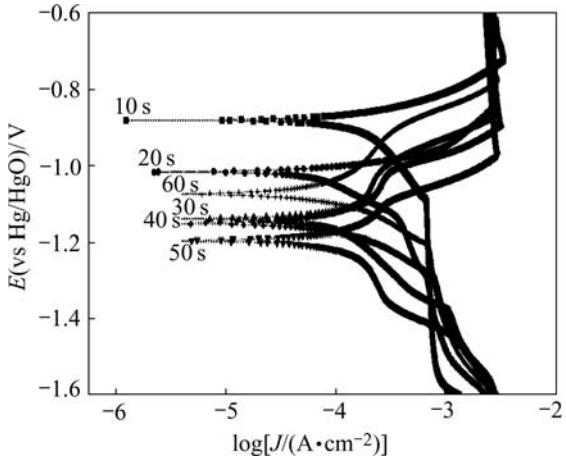

Fig.5 Tafel polarization curves of zincate films in 3.5%NaCl at different zincate times

Table 3 Fitting results of Tafel polarization curves in 3.5%NaCl at different zincate times

Zincate time/s	E_{corr}(vs Hg/HgO)/V	$J_{coor}/(10^{-4}A\cdot cm^{-2})$
10	-0.881	3.388
20	-1.017	2.483
30	-1.139	2.298
40	-1.196	2.093
50	-1.151	2.232
60	-1.075	1.819

From Fig.5 and Table 3, content of Zn is low at the beginning of zincate process, and large area of Al-Si alloy surface is bare, thus the corrosion current is high. With the increase of zincate time, Al-Si alloy is covered by zinc layer gradually, leading to the decrease in corrosion current. At 60 s, corrosion current reaches its minimum, and corrosion current varies slightly during 20−60 s. Corrosion potential shifts negatively with the increase of zincate time, which reaches its minimum at 40 s and then increases gradually, indicating that the surface is fully covered by zinc layer after 40 s.

2) Tafel polarization curves of zinc layers in zincate solution

Tafel polarization curves of zinc layers on Al-Si alloy attained from non-cyanide multi-metal zincate solution were tested in zincate solution, as shown in Fig.6, and the fitting results are listed in Table 4.

It can be seen from Fig.6 and Table 4 that corrosion potential descends from the beginning to 30 s, and increases after 30 s, varies slightly after 40 s, indicating

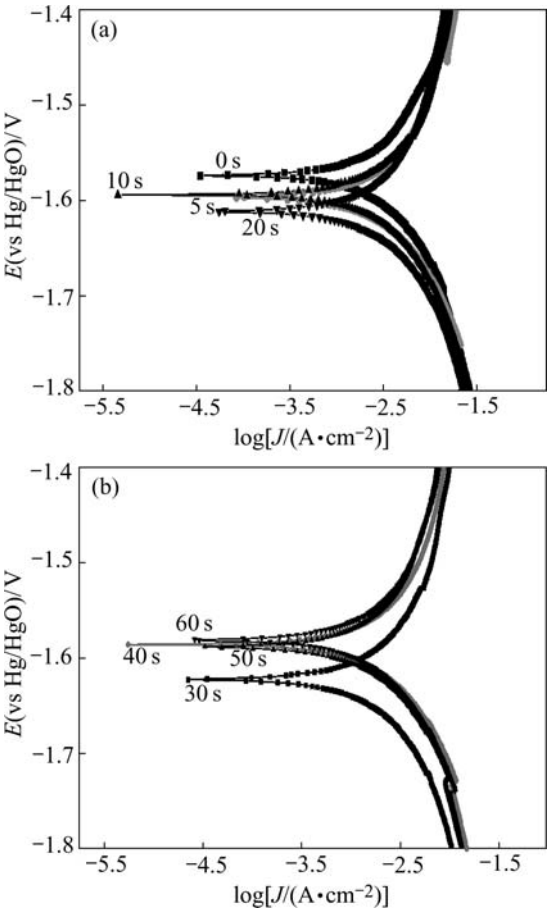

Fig.6 Tafel polarization curves of zincate films in zincate solution at different zincate times

Table 4 Fitting results of Tafel polarization curves of zincate films in zincate solution at different zincate times

Zincate time/s	E_{corr}(vs Hg/HgO)/V	$J_{coor}/(10^{-3}A\cdot cm^{-2})$
0	-1.574	5.223
5	-1.597	5.414
10	-1.594	5.864
20	-1.612	6.141
30	-1.622	5.588
40	-1.585	5.307
50	-1.587	5.194
60	-1.580	5.158

that the surface is fully covered by zinc layer after 40 s. $E^{3+}_{Al/Al} < E^{2+}_{Al/Zn} < E^{2+}_{Zn/Zn}$, which means that Al is dissolved at the beginning of zincate process. From the beginning to 20 s, corrosion current increases gradually, due to the corrosion of Al. After that, the corrosion current descends, mainly due to the deposit of zinc.

3) *E*—*t* curves of zinc layers at different zincate times

E—*t* curves of zinc layers at different zincate times are shown in Fig.7, and relationship between the lowest potential and zincate time from *E*—*t* curve is displaced in Fig.8. From the *E*—*t* curves of zinc layers in Fig.7, it

is found that electrode potential descends at the beginning, referring to the dissolution of Al. The electrode potential increases and finally reaches a stable value after its minimum. Fig.8 shows that the lowest potential decreases in the first 30 s and reaches its minimum at 30 s, while an increase is seen from 30 s to 60 s, indicating that dissolution of Al is decreased due to the coverage of Zn on the surface of Al-Si alloy.

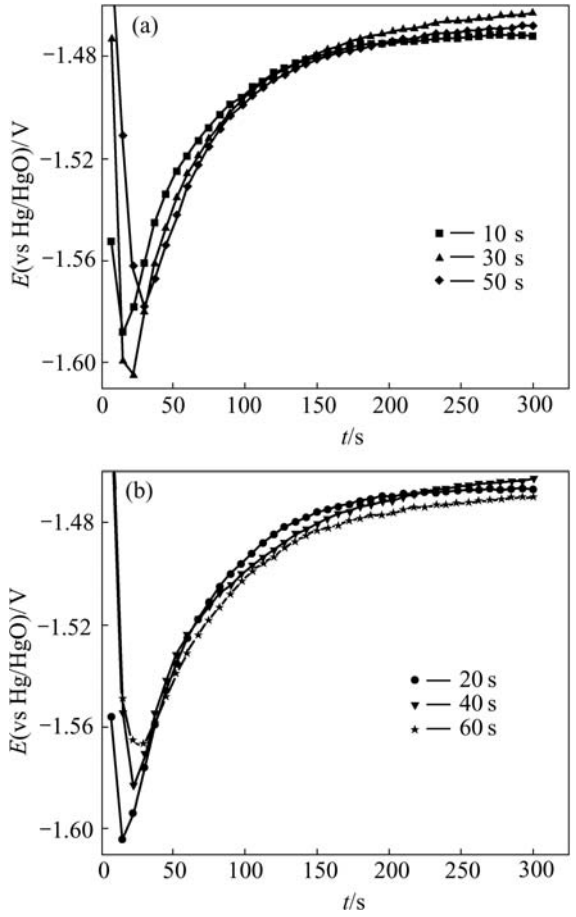

Fig.7 E—t curves of zincate films in zincate solution at different zincate times

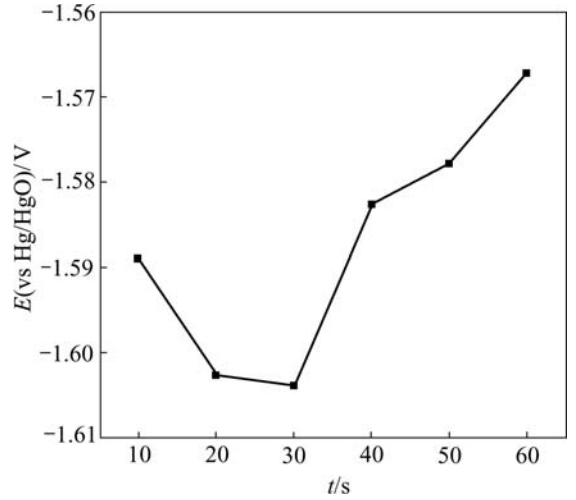

Fig.8 Relationship between the lowest potential and zincate time

4) E—t curves of Al-Si alloy, Zn, Fe, Ni, Cu, zincate layer in mixture of NaOH solution and composite complexing agents

E—t curves of Al-Si alloy, Zn, Fe, Ni, Cu, zincate layer in a mixture of NaOH solution and composite complexing agents were tested to investigate the change of surface structure of the Al-Si alloy, shown in Fig.9, and the stable potentials at 240 s are listed in Table 5.

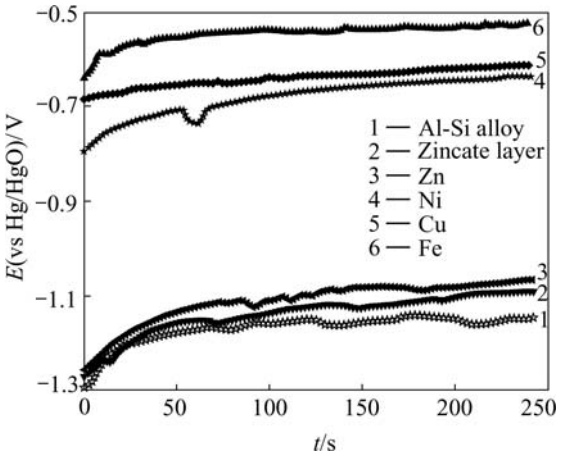

Fig.9 E—t curves of Al-Si alloy, Zn, Fe, Ni, Cu, zincate layer in mixture of NaOH solution and composite complexing agents

Table 5 Stable potential of different samples after 240 s zincate

Sample	E(vs Hg/HgO)/V
Al-Si alloy	−1.149 0
Zincate layer	−1.093 0
Zn	−1.068 0
Ni	−0.636 1
Cu	−0.613 8
Fe	−0.523 7

Stable potential of Al-Si alloy is −1.149 0 V, and that of Zn is −1.068 0 V, indicating that the potential will shift positively when Al-Si alloy surface is covered by zincate layer. Practically, stable potential of Al-Si alloy covered by zincate layer is −1.093 0 V, indicating that the zincate layer is very thin, however, it's the thin film that inhibits the growth of oxide film on Al-Si alloy, and provides a fine substrate for further electrochemical plating or chemical plating.

5) Relationship between zincate layer coverage and potential

At the beginning of the zincate process, discontinuous zinc alloy crystals grew on the Al-Si alloy surface. With the increase of zincate time, the zincate film became denser, and the surface would be fully covered by zincate film after 30 s. Theoretically, the substrate could not be fully covered by zincate film, for anodic reaction (dissolution of Al) always exists in replacement reaction. Therefore, some fine holes on the

zincate film were generated for the corrosion of Al. Compared with the area of the zincate layer, the holes could be ignored and the coverage θ was assumed to be 1, thus the relationship between the zincate layer coverage θ and potential E can be described as

$$\theta=aE+b(a \text{ and } b \text{ are constants}) \quad (9)$$

when θ=0, E_0=−1.574 V; θ=1, E_1=−1.622 V. Therefore, formula (9) becomes

$$\theta=-20.833E-32.792 \quad (10)$$

6) EIS analysis of zincate process

EIS was firstly applied to study the zincate process. Due to the complicated and the fast reaction in zincate process, a mixture of NaOH and ZnO was used as the zincate solution. EIS of pure Zn and pure Al in zincate solution are shown in Figs.10 and 11 respectively.

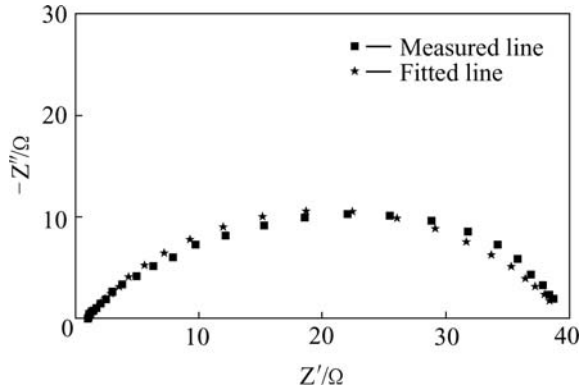

Fig.10 EIS spectra for pure zinc in zincate solution

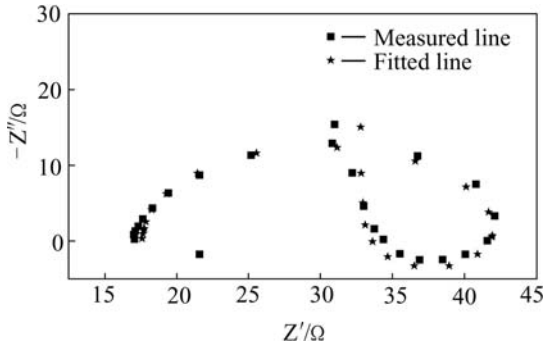

Fig.11 EIS of pure aluminum in zincate solution

A large captance circle at high frequency is seen in the EIS of pure Zn, which is due to the electric double layer capacitance and electrochemical resistance, indicating that there is only one time constant, referring to the deposition of Zn. EIS of pure Al is more complicated, with a captance arc at high frequency, an inductive reactance arc at mediate-low frequency.

Equivalent circuit models for pure zinc and pure aluminum in zincate solution are shown in Fig.12, and the fitting results are listed in Tables 6 and 7.

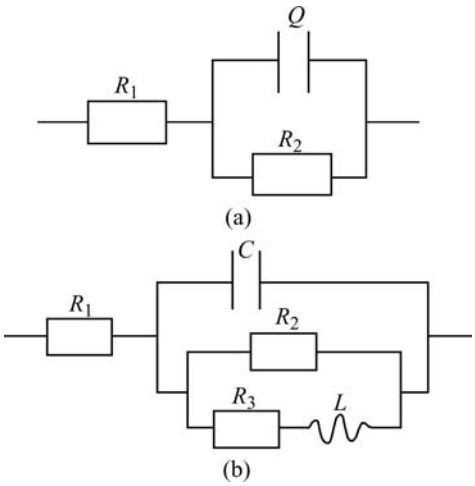

Fig.12 Equivalent circuit models for pure zinc(a) and pure aluminum(b) in zincate solution

Table 6 Circuit parameters for pure zinc in simple zincate solution

R_1/Ω	R_2/Ω	Q/F	n
1.097 5	3.856 7	$2.077\ 8\times10^{-3}$	0.641 2

Table 7 Circuit parameter for pure aluminum in simple zincate solution

R_1/Ω	C/F	R_2/Ω	R_2/Ω	L/Ω
17.626	$4.086\ 7\times10^{-3}$	24.946	38.640	0.192 1

It can be seen that electrochemical resistance R_1 of pure Al is much larger than that of pure Zn, indicating that the corrosion of Al in zincate process cannot be neglected. The inductive reactance arc at mediate frequency of pure Al may be caused by adsorption on the surface of the substrate covered by zincate film. With the increasing protection of zincate film, reaction resistance increases for further zincate, appeared as the increase in the radius of captance arc at high-intermediate frequency. With the growth of the zincate film, inductive reactance increases. The adsorption on the surface may be attributed by the formation of $Al(OH)_3$ in alkaline zincate solution in the final period of zincate process.

4 Conclusions

1) The apparent activation energy of cast Al-Si alloy in non-cyanide multi-metal zincate solution was calculated from Arrhenius formula.

2) From the standard electrode potential of metal ions in zincate solution and electromotive force of replacement reaction replacement reaction in multi-metal zincate solution, it is shown that Cu^{2+}, Ni^{2+}, Fe^{2+} and then Zn^{2+} could be co-deposited in multi-metal zincate solution. Galvanic couple order of Al-Si alloy, Zn, Fe, Ni

and Cu in multi-metal zincate solution is Cu＞Ni＞Fe＞Zn>Al-Si alloy.

3) Tafel polarization curves and *E*—*t* curves show that corrosion potential descends with the increase of zincate time, while ascends in 30 s to 40 s. The coverage of zincate layer on the Al-Si alloy substrate is rather large after 30−40 s.

4) EIS shows inductive reactance arc at the mediate-low frequency in zincate process, due to the adsorption on the surface of the substrate covered by zincate film.

References

[1] VINARCIK E J. Light metal advances in the Automotive industry(Part Ⅱ): aluminium[J]. Light Metal ACE, 2001, 6: 22−27.

[2] CACERES C H, WANG L. Alloy selection for die castings using the quality index[J]. AFS Transactions, 1999, 147: 239−247.

[3] ZHAO Ai-min, MAO Wei-min, ZHEN Zi-sheng, JIANG Chun-mei, ZHONG Xue-you. Effects of cooling rate on solidification microstructures and wear resistance of hypereutectic Al-Si alloy[J]. The Chinese Journal of Nonferrous Metals, 2001, 11(5): 827−832.(in Chinese)

[4] HAWKE D, RUDEN T. Magnesium in vehicle design[J]. Society of Automotive Engineers, 1995: 63.

[5] ISACSSON M, STROM M, ROOTZEN H, LUNDER O. Galvanically induced atmospheric corrosion on magnesium alloys: a designed experiment evaluated by extreme value statistics and conventional techniques[J]. SAE Special Publications, 1997, 1250: 43−55.

[6] XU Rui-dong, GUO Zhong-cheng, XUE Fang-qin, WANG Jun-li. Electrodeposited Re-Ni-W-P-SiC composite ceramic coating on cast aluminium containing high silicon[J]. New Technology & New Technics, 2002, 11: 37−39.

[7] YUAN Shun-de, CHEN Tian-chu. Electroplating for casting aluminium alloy[J]. Electroplating & Pollution Control, 2002, 22(3): 39−40.

[8] SHEN Ya-guang. Electroplating for aluminium alloy hub[J]. Electroplating & Pollution Control, 2003, 23(1): 12−15.

[9] LIU Lian-hua, ZHANG Sheng-da, WANG Ru-xing. The technics of high speed hard chromium plating for casting aluminium cylinder[J]. Electroplating & Pollution Control, 2002, 22(6): 3−4.

[10] XIN Jia-nan. Electroless nickel plating process for aluminium alloy hub[J]. Electroplating & Finishing, 2001, 20(5): 25−27.

[11] TANG Chun-hua. Discussion of aluminum hub plating technology[J]. Automobile Technology & Material, 2001, 11: 17−19.

[12] LASHMORE D S. Immersion deposit pretreatments for electroplating on aluminium[J]. Plating & Surface Finishing, 1978, 4: 44−47.

[13] STOYANOVA E, STOYCHEV D. Electrochemical aspects of the immersion treatment of aluminium[J]. Journal of Applied Electrochemistry, 1997, 27: 684−689.

[14] ROBERTSON S G, RITCHIE I M. A kinetic and electrochemical study of the zincate immersion process for aluminium[J]. Journal of Applied Electrochemistry, 1995, 25: 659−666.

[15] PARAMASIVAM M, VENKATAKRISHNA IYER S, KAPALI V. Effect of zincate conversion coating on corrosion and anodic behaviour of commercial aluminium in alkaline media[J]. British Corrosion Journal, 1994, 29(3): 207−208.

[16] TANG Y C, DAVENPORT A J. The effect of heat treatment and surface roughness on the zincate Treatment of aluminium alloy 6082[J]. Trans IMF, 2001, 79(3): 85−89.

[17] LIANG M W, HSIEH T E, CHEN C C, HUANG Y T. Electroless copper/nickel films deposited on AlN substrates[J]. Japanese Journal of Applied Physics, 2004, 43(12): 8258−8266.

[18] PEARSON T, WAKE S. Verbesserungen bei der vorbehandlung von aluminium als substrat fuer die galvanische abscheidung[J]. Galvanotechnik, 2000, 91(11): 3054−3061.

(Edited by LI Xiang-qun)